Asia Pac. J. Math. 2026 **13**:111

STABILITY AND HOPF BIFURCATION ANALYSIS OF AN HIV/AIDS MODEL WITH VERTICAL TRANSMISSION, NONLINEAR INCIDENCE AND TREATMENT COMPLETION DELAY

JAY MICHAEL R. MACALALAG

Department of Mathematics, Caraga State University, Philippines

jrmacalalag@carsu.edu.ph

Received May 7, 2026

Abstract. This paper studies a delay differential equation model for HIV/AIDS transmission that incorporates vertical transmission, a saturated nonlinear incidence rate, movement to safer sexual practices, and a discrete delay in treatment completion. We derive the basic reproduction number and establish threshold conditions for disease invasion. A sufficient condition guaranteeing positivity and boundedness of solutions is presented, the disease-free equilibrium is characterized through the associated infected subsystem, and the endemic equilibrium is shown to exist whenever the reproduction number exceeds one. For the endemic state, the linearized problem reduces to a transcendental characteristic equation of the form $P(\lambda) + Q(\lambda)e^{-\lambda\tau} = 0$ which allows us to obtain explicit local stability conditions when the delay is absent and to derive a Hopf bifurcation criterion when the delay varies. The numerical section is expanded to include time-series plots, a phase portrait, additional intervention-oriented scenarios, and a local sensitivity analysis of the most influential parameters. The simulations show that short treatment delays preserve convergence to the endemic equilibrium, while sufficiently long delays generate oscillatory instability in the infectious classes.

2020 Mathematics Subject Classification. 34K20; 34K18; 34D20; 37G15; 92D30.

Key words and phrases. HIV/AIDS; nonlinear incidence; vertical transmission; delay differential equations; stability; Hopf bifurcation.

1. Introduction

HIV/AIDS remains a persistent public health concern, not only because of continued sexual transmission but also because of mother-to-child transmission, treatment interruption, and the long clinical pathway from infection to AIDS. These features make HIV dynamics particularly suitable for delay models: treatment effects are rarely instantaneous, and the epidemiological consequences of treatment completion or failure often appear after a waiting period.

DOI: 10.28924/APJM/13-111

Mathematical models help identify the mechanisms that matter most. In the present work, we consider a five-compartment HIV/AIDS system consisting of susceptible individuals $S(t)$, individuals practicing safer sexual behavior $R(t)$, HIV-positive individuals $I(t)$, treated individuals $T(t)$, and individuals with AIDS $A(t)$. The incidence term is taken to be saturated in order to reflect a contact process that does not grow linearly without bound when the interacting classes become large. We also incorporate vertical transmission and allow treated individuals to leave treatment only after a discrete time lag.

Recent HIV modeling studies have moved beyond classical compartmental formulations by incorporating richer biological and epidemiological mechanisms. For example, Wang et al. [1] studied an HIV infection model with two time delays and obtained stability-switch and Hopf bifurcation results for the infected equilibrium. Wu et al. [2] analyzed an age-since-infection diffusion HIV/AIDS model with treatment adherence, while Zhang et al. [3] investigated an age-space structured HIV model with latency and established both local and global stability results. At the population level, Chazuka et al. [4] showed how imperfect pre-exposure prophylaxis can produce backward bifurcation, and AlShamrani et al. [5] examined the influence of immune impairment and multiple infection pathways in generalized HIV-1 systems. The work of Lahmidani et al. [6] analyzed an HIV model with two saturated rates, CTL response, and therapy; this is especially relevant to the present study because it reinforces the mathematical importance of saturation effects in HIV transmission and treatment dynamics. More recently, Li et al. [7] developed an infection-age HIV model with delayed immune response and data fitting, whereas Marsudi et al. [8] and Sado et al. [9] emphasized bifurcation, sensitivity, and optimal control issues in HIV/AIDS transmission models.

This work also connects with earlier time delay-based HIV/AIDS modeling that incorporated vertical transmission. In particular, the study of Teng et al. [10] highlighted how delayed mechanisms and mother-to-child transmission can alter threshold dynamics and stability. Motivated by these developments, we focus here on a model that combines vertical transmission, safer-sex behavior, saturated incidence, and a treatment-completion delay in a single analytical framework.

The main contribution of this paper is the analytical treatment of an HIV/AIDS model that simultaneously incorporates saturated incidence, vertical transmission, safer-sex transition, and a treatment-completion delay. We derive the threshold quantity, characterize the disease-free and endemic equilibria, obtain local stability conditions, and identify a delay-induced Hopf bifurcation mechanism. Numerical simulations are then used to illustrate the theoretical results.

2. Model formulation

Let $S(t)$, $R(t)$, $I(t)$, $T(t)$, and $A(t)$ denote, respectively, the number of susceptible individuals, individuals practicing safer sexual behavior, HIV-positive infectious individuals, treated individuals,

and individuals with AIDS at time $t \geq 0$. New individuals enter the susceptible class at rate $\pi > 0$. Transmission from susceptible to infected individuals is governed by the saturated incidence

$$\mathcal{I}(S, I) = \frac{\beta SI}{1 + aS + bI}, \qquad \beta > 0, \quad a \geq 0, \quad b \geq 0.$$

Here, parameters a and b describe the saturation effects due to susceptible individuals and infected individuals, respectively. These parameters prevent the incidence from increasing without bound as S and I become large. Biologically, they account for limited effective contacts, behavioral adaptation, awareness of HIV risk, and preventive responses that reduce the actual number of successful transmissions.

Susceptible individuals adopt safer sexual practices at rate γ and move to the class R. Natural mortality occurs at rate μ in every compartment. Infected individuals start treatment at rate r, progress to AIDS at rate ζ, and experience disease-induced mortality at rate ε_1. Treated individuals experience disease-induced mortality at rate ε_3, while individuals with AIDS die at rate ε_2.

Vertical transmission is represented by an additional infected recruitment term $(1 - \varepsilon)\theta I$, where $\theta \geq 0$ denotes the transmission potential and $\varepsilon \in [0, 1]$ measures the effectiveness of preventing mother-to-child transmission. A discrete delay $\tau \geq 0$ is introduced in the treatment completion term: at time t, the rate at which individuals leave treatment depends on the treated population τ time units earlier. The term $\alpha T(t - \tau)$ represents treatment completion at time t by individuals who were in the treated class τ time units earlier. Hence, the delay describes the required treatment duration before completion outcomes are realized. Because this delayed outflow depends on the past treated population, the model is studied under biologically admissible histories that preserve the nonnegativity of the treated compartment. A proportion $k \in [0, 1]$ of those individuals returns to the infectious class, while the remaining fraction $1 - k$ progresses to AIDS.

The resulting system is given by

$$\begin{aligned}
\frac{dS}{dt} &= \pi - \frac{\beta SI}{1 + aS + bI} - \gamma S - \mu S, \\
\frac{dI}{dt} &= \frac{\beta SI}{1 + aS + bI} + (1 - \varepsilon)\theta I + k\alpha T(t - \tau) - (\zeta + r + \mu + \varepsilon_1)I, \\
\frac{dT}{dt} &= rI - \alpha T(t - \tau) - (\mu + \varepsilon_3)T, \\
\frac{dA}{dt} &= \zeta I + (1 - k)\alpha T(t - \tau) - (\mu + \varepsilon_2)A, \\
\frac{dR}{dt} &= \gamma S - \mu R.
\end{aligned} \tag{1}$$

TABLE 1. Description of model parameters

Parameter	Description	Admissible Values
π	Recruitment rate into the susceptible class	$(0, \infty)$
β	Effective transmission rate for HIV infection	$(0, \infty)$
γ	Rate at which susceptible individuals adopt safer sexual behavior	$(0, \infty)$
ζ	Progression rate from HIV infection to AIDS	$(0, \infty)$
θ	Vertical-transmission potential	$(0, \infty)$
ε_1	Disease-induced death rate of HIV-positive infectious individuals	$(0, \infty)$
ε_2	Disease-induced death rate of individuals with AIDS	$(0, \infty)$
ε_3	Disease-induced death rate of treated individuals	$(0, \infty)$
μ	Natural death rate	$(0, \infty)$
a	Saturation parameter associated with the susceptible population	$[0, \infty)$
b	Saturation parameter associated with the infected population	$[0, \infty)$
r	Treatment initiation rate of HIV-positive infectious individuals	$(0, \infty)$
α	Treatment-completion rate	$(0, \infty)$
ε	Effectiveness of prevention of mother-to-child transmission	$[0, 1]$
k	Fraction of treated individuals returning to the infectious class after treatment completion	$[0, 1]$

The delay term $T(t-\tau)$ represents a treatment-completion loss rate determined by the treated population τ period earlier. Since this delayed loss may, in principle, exceed the currently available treated population, the delayed-loss formulation is considered only for admissible initial histories and parameter values for which the treated compartment remains nonnegative. This admissibility condition is consistent with the biological requirement that all state variables remain nonnegative. Although an alternative quasipositive formulation could use the current loss $-\alpha T(t)$ in the treated equation while retaining delayed completion inflows in the I and A equations, such a modification would lead to a different dynamics. Hence, this study retains the delayed-loss formulation and explicitly imposes the admissibility condition needed for biological feasibility.

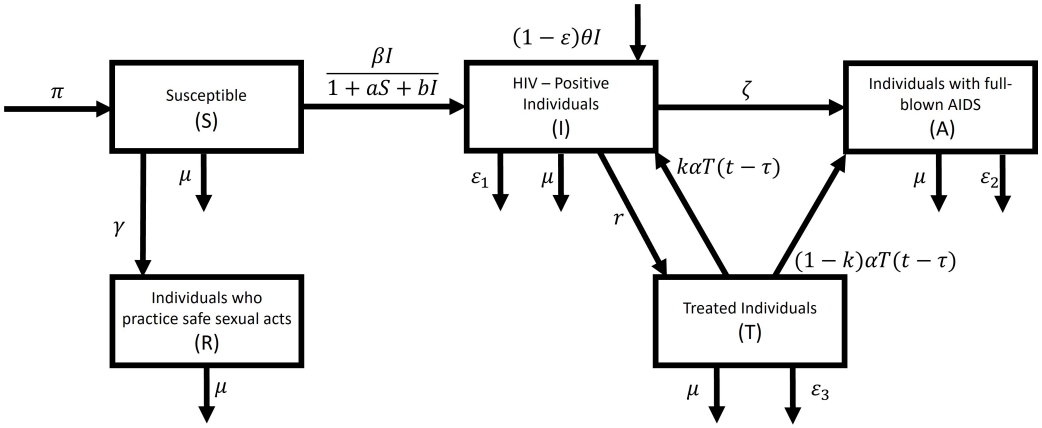

FIGURE 1. Model Diagram of HIV/AIDS Infection

To determine the solution for $t \geq 0$, we prescribe continuous initial histories on $[-\tau, 0]$ using the same ordering as the model equations, namely (S, I, T, A, R):

$$(S(\theta), I(\theta), T(\theta), A(\theta), R(\theta)) = (\phi_1(\theta), \phi_2(\theta), \phi_3(\theta), \phi_4(\theta), \phi_5(\theta)), \qquad \theta \in [-\tau, 0], \tag{2}$$

with $\phi_i(\theta) \geq 0$ for all $\theta \in [-\tau, 0]$.

3. Well-posedness and a positively invariant region

Let $\mathcal{C} = C([-\tau, 0], \mathbb{R}^5)$ and $\mathcal{C}_+ = C([-\tau, 0], \mathbb{R}^5_+)$. We use the ordering (S, I, T, A, R) and write

$$N(t) = S(t) + I(t) + T(t) + A(t) + R(t)$$

for the total population size.

The only nonstandard point in the positivity argument is the delayed loss term $-\alpha T(t-\tau)$ in the treated equation. Since this term is not quasipositive, nonnegative histories alone do not guarantee that $T(t)$ remains nonnegative. We, therefore, call a nonnegative history *admissible* if the corresponding method-of-steps solution satisfies the boundary compatibility condition

$$\alpha T(t-\tau) \leq rI(t) \qquad \text{whenever } T(t) = 0. \tag{3}$$

Biologically, condition (3) ensures that the delayed treatment-completion outflow does not exceed the current inflow of infected individuals into treatment when the treated class is depleted.

Lemma 3.1. *Assume that the initial history is admissible and nonnegative. Let*

$$\nu = (1 - \varepsilon)\theta$$

and suppose that

$$\delta = \mu - \max\{\nu - \varepsilon_1, 0\} > 0.$$

Then system (1) has a unique global solution which remains nonnegative and bounded for all $t \geq 0$. Moreover, the set

$$\Omega_\delta = \left\{ \phi \in C([-\tau, 0], \mathbb{R}^5_+) : \sum_{j=1}^{5} \phi_j(\theta) \leq \frac{\pi}{\delta},\ \theta \in [-\tau, 0] \right\}$$

is positively invariant.

Proof. The right-hand side of system (1) is continuous, locally Lipschitz in the present state variables, and depends continuously on the delayed term $T(t-\tau)$. Hence, by the standard theory of retarded functional differential equations, a unique local solution exists for every initial history in $C([-\tau, 0], \mathbb{R}^5)$.

We first verify nonnegativity. On the boundary $S = 0$, we have

$$S'(t) = \pi > 0.$$

If $I(t) = 0$, then

$$I'(t) = k\alpha T(t-\tau) \geq 0.$$

If $A(t) = 0$, then

$$A'(t) = \zeta I(t) + (1-k)\alpha T(t-\tau) \geq 0,$$

and if $R(t) = 0$, then

$$R'(t) = \gamma S(t) \geq 0.$$

For the treated class, the delayed-loss term is not quasipositive. Therefore, by the admissibility condition,

$$\alpha T(t-\tau) \leq rI(t) \qquad \text{whenever } T(t) = 0,$$

we obtain

$$T'(t) = rI(t) - \alpha T(t-\tau) \geq 0 \qquad \text{whenever } T(t) = 0.$$

Thus, no component can cross from the nonnegative cone into the negative region, and the solution remains nonnegative as long as it exists.

Now, let

$$N(t) = S(t) + I(t) + T(t) + A(t) + R(t).$$

Adding all equations in (1), the incidence terms, safer-sex transition terms, treatment-initiation terms, progression terms, and delayed treatment-completion terms cancel. Hence,

$$N'(t) = \pi + (1-\varepsilon)\theta I(t) - \mu N(t) - \varepsilon_1 I(t) - \varepsilon_2 A(t) - \varepsilon_3 T(t).$$

Equivalently, with $\nu = (1-\varepsilon)\theta$,

$$N'(t) = \pi - \mu N(t) - (\varepsilon_1 - \nu) I(t) - \varepsilon_2 A(t) - \varepsilon_3 T(t).$$

Since all state variables are nonnegative and $I(t) \leq N(t)$, we have

$$N'(t) \leq \pi - \mu N(t) + \max\{\nu - \varepsilon_1, 0\} I(t).$$

Therefore,

$$N'(t) \leq \pi - [\mu - \max\{\nu - \varepsilon_1, 0\}] N(t).$$

By the definition of δ, this becomes

$$N'(t) \leq \pi - \delta N(t).$$

The comparison theorem gives

$$N(t) \leq N(0)e^{-\delta t} + \frac{\pi}{\delta}\left(1 - e^{-\delta t}\right).$$

Hence,

$$N(t) \leq \max\left\{N(0), \frac{\pi}{\delta}\right\},$$

so all components are bounded. Boundedness rules out finite-time blow-up, and therefore the local solution extends globally.

Finally, if the initial history belongs to Ω_δ, then

$$N(\theta) \le \frac{\pi}{\delta}, \qquad \theta \in [-\tau, 0].$$

The comparison estimate implies

$$N(t) \le \frac{\pi}{\delta} \qquad \text{for all } t \ge 0.$$

Thus, the solution remains in Ω_δ for all $t \ge 0$, and Ω_δ is positively invariant. □

Remark 3.2. Let $c = \mu + \varepsilon_3$. A first-step sufficient condition for the treated component is obtained by assuming

$$\alpha\big(e^{c\tau} - 1\big) \le c, \tag{4}$$

together with the initial bound

$$0 \le \phi_3(\theta) \le \phi_3(0), \qquad \theta \in [-\tau, 0]. \tag{5}$$

Indeed, on $[0, \tau]$ the treated equation implies

$$T(t) \ge \phi_3(0)e^{-ct}\left[1 - \frac{\alpha}{c}\big(e^{ct} - 1\big)\right],$$

so (4) ensures that $T(t) \ge 0$ on $[0, \tau]$. This estimate provides a sufficient positivity condition on the first delay interval. For subsequent intervals, nonnegativity of the treated class still depends on the admissibility condition (3), since the delayed treatment-completion term must not exceed the number of treated individuals available after ordinary depletion during one delay period. Biologically, condition (4) requires that the delayed completion pressure remains compatible with the treated population that survives over the delay interval.

4. Equilibria and the basic reproduction number

At equilibrium, the delayed term satisfies $T(t - \tau) = T^*$. Hence, the steady-state equations are

$$0 = \pi - \frac{\beta SI}{1 + aS + bI} - (\gamma + \mu)S, \tag{6a}$$

$$0 = \frac{\beta SI}{1 + aS + bI} + (1 - \varepsilon)\theta I + k\alpha T - (\zeta + r + \mu + \varepsilon_1)I, \tag{6b}$$

$$0 = rI - (\alpha + \mu + \varepsilon_3)T, \tag{6c}$$

$$0 = \zeta I + (1 - k)\alpha T - (\mu + \varepsilon_2)A, \tag{6d}$$

$$0 = \gamma S - \mu R. \tag{6e}$$

4.1. **Disease-free equilibrium.** Setting $I = T = A = 0$ in (6) yields the disease-free equilibrium, written in the order (S, I, T, A, R),

$$E_0 = (S_0, 0, 0, 0, R_0), \qquad S_0 = \frac{\pi}{\gamma + \mu}, \qquad R_0 = \frac{\gamma}{\mu} S_0. \tag{7}$$

4.2. **Basic reproduction number.** In solving for the basic reproduction number, we used the next-generation matrix approach of van den Driessche and Watmough [11]. Let the infected variables be (I, T). At the disease-free equilibrium, the new-infection and transition matrices are

$$F = \begin{pmatrix} \dfrac{\beta S_0}{1 + aS_0} + (1 - \varepsilon)\theta & 0 \\ 0 & 0 \end{pmatrix}, \qquad V = \begin{pmatrix} \zeta + r + \mu + \varepsilon_1 & -k\alpha \\ -r & \alpha + \mu + \varepsilon_3 \end{pmatrix}.$$

Since

$$\det V = (\zeta + r + \mu + \varepsilon_1)(\alpha + \mu + \varepsilon_3) - k\alpha r > 0,$$

the next-generation matrix FV^{-1} has spectral radius

$$\rho(FV^{-1}) = \frac{\dfrac{\beta S_0}{1 + aS_0} + (1 - \varepsilon)\theta}{(\zeta + r + \mu + \varepsilon_1) - \dfrac{k\alpha r}{\alpha + \mu + \varepsilon_3}}.$$

Thus, the basic reproduction number is

$$\mathcal{R}_0 = \frac{\dfrac{\beta\pi}{\gamma + \mu + a\pi} + (1 - \varepsilon)\theta}{(\zeta + r + \mu + \varepsilon_1) - k\alpha \dfrac{r}{\alpha + \mu + \varepsilon_3}}. \tag{8}$$

Equivalently,

$$\mathcal{R}_0 = \frac{(\alpha + \mu + \varepsilon_3)\left[\beta\pi + (1 - \varepsilon)\theta(\gamma + \mu + a\pi)\right]}{(\gamma + \mu + a\pi)\left[(\zeta + r + \mu + \varepsilon_1)(\alpha + \mu + \varepsilon_3) - k\alpha r\right]}.$$

Remark 4.1. Since $\zeta + r + \mu + \varepsilon_1 > r$, $\alpha + \mu + \varepsilon_3 > \alpha$, and $0 \le k \le 1$, we have

$$(\zeta + r + \mu + \varepsilon_1)(\alpha + \mu + \varepsilon_3) - k\alpha r > 0.$$

Thus, the denominator of $\mathcal{R}_0$ is positive. Moreover, the numerator is positive under the stated parameter assumptions. Hence, $\mathcal{R}_0 > 0$.

The delay τ does not appear in $\mathcal{R}_0$ because the threshold is obtained from the zero-growth balance of the infected subsystem at the disease-free state.

4.3. **Endemic equilibrium.** For any endemic equilibrium $E^* = (S^*, I^*, T^*, A^*, R^*)$ with $I^* > 0$, equations (6c)–(6e) give

$$T^* = \frac{r}{\alpha+\mu+\varepsilon_3} I^*, \qquad A^* = \frac{\zeta I^* + (1-k)\alpha T^*}{\mu+\varepsilon_2}, \qquad R^* = \frac{\gamma}{\mu} S^*. \tag{9}$$

Define

$$D = (\zeta + r + \mu + \varepsilon_1) - (1-\varepsilon)\theta - k\alpha \frac{r}{\alpha+\mu+\varepsilon_3}. \tag{10}$$

Theorem 4.2. *Assume that*

$$D > 0 \qquad \textit{and} \qquad \beta > aD.$$

Then system (1) has a unique positive endemic equilibrium if and only if $\mathcal{R}_0 > 1$. Whenever it exists, the endemic equilibrium is given by

$$I^* = \frac{(\beta - aD)\pi - (\gamma+\mu)D}{D\big[(\beta - aD) + (\gamma+\mu)b\big]}, \qquad S^* = \frac{D + b\pi}{(\beta - aD) + (\gamma+\mu)b}, \tag{11}$$

$$T^* = \frac{r\big[(\beta - aD)\pi - (\gamma+\mu)D\big]}{(\alpha+\mu+\varepsilon_3)D\big[(\beta - aD) + (\gamma+\mu)b\big]}, \tag{12}$$

$$A^* = \frac{\big[\zeta(\alpha+\mu+\varepsilon_3) + (1-k)\alpha r\big]\big[(\beta - aD)\pi - (\gamma+\mu)D\big]}{(\mu+\varepsilon_2)(\alpha+\mu+\varepsilon_3)D\big[(\beta - aD) + (\gamma+\mu)b\big]}, \qquad R^* = \frac{\gamma(D + b\pi)}{\mu\big[(\beta - aD) + (\gamma+\mu)b\big]}. \tag{13}$$

Proof. Let $E^* = (S^*, I^*, T^*, A^*, R^*)$ be an endemic equilibrium. Since $I^* > 0$, equation (6c) gives

$$T^* = \frac{r}{\alpha+\mu+\varepsilon_3} I^*.$$

Substitution into (6d) and (6e) gives (9).

Dividing (6b) by $I^* > 0$ and using (9) gives

$$\frac{\beta S^*}{1 + aS^* + bI^*} = D.$$

Therefore,

$$\beta S^* = D(1 + aS^* + bI^*), \tag{14}$$

and, because $D > 0$ and $\beta > aD$,

$$S^* = \frac{D(1 + bI^*)}{\beta - aD}. \tag{15}$$

Using (14) in (6a) yields

$$0 = \pi - DI^* - (\gamma+\mu)S^*.$$

Substituting (15) gives

$$(\beta - aD)\pi = D\big[(\beta - aD) + (\gamma+\mu)b\big]I^* + (\gamma+\mu)D.$$

This proves the formula for I^* in (11), and substitution into (15) gives the formula for S^*. The expressions for T^*, A^*, and R^* follow from (9); hence the endemic equilibrium is unique.

It remains to characterize positivity. Since $D > 0$ and $\beta > aD$, the denominator in (11) is positive. Thus $I^* > 0$ if and only if

$$(\beta - aD)\pi > (\gamma + \mu)D.$$

Equivalently,

$$\frac{\beta\pi}{\gamma + \mu + a\pi} > D.$$

Using the definition of D, this is precisely

$$\frac{\beta\pi}{\gamma + \mu + a\pi} + (1 - \varepsilon)\theta > (\zeta + r + \mu + \varepsilon_1) - k\alpha\frac{r}{\alpha + \mu + \varepsilon_3},$$

which is equivalent to $\mathcal{R}_0 > 1$ by (8). Hence the endemic equilibrium is positive if and only if $\mathcal{R}_0 > 1$. □

5. Local stability of the disease-free and endemic equilibria

5.1. **Disease-free equilibrium.**

We examine the local stability of the disease-free equilibrium E_0 by linearizing (1) at E_0.

Theorem 5.1. *The disease-free equilibrium E_0 has the following stability properties.*

(*i*) *If $\tau = 0$ and $\mathcal{R}_0 < 1$, then E_0 is locally asymptotically stable.*

(*ii*) *If $\mathcal{R}_0 > 1$, then E_0 is unstable for every $\tau \geq 0$.*

(*iii*) *If $\mathcal{R}_0 < 1$ and $\tau > 0$, stability can be lost only through positive roots ω of*

$$(\omega^2 + c^2)(\omega^2 + d^2) - \alpha^2\{\omega^2 + (c + kr)^2\} = 0, \tag{16}$$

where

$$c = \frac{\beta S_0}{1 + aS_0} + (1 - \varepsilon)\theta - (\zeta + r + \mu + \varepsilon_1), \qquad d = \mu + \varepsilon_3.$$

In particular, if (16) has no positive root, then no Hopf crossing occurs from the infected subsystem and the disease-free equilibrium remains locally stable for the delays considered.

Proof. Let

$$c = \frac{\beta S_0}{1 + aS_0} + (1 - \varepsilon)\theta - (\zeta + r + \mu + \varepsilon_1), \qquad d = \mu + \varepsilon_3.$$

The characteristic equation of the infected subsystem at E_0 is

$$\Delta_0(\lambda) = (\lambda - c)\big(\lambda + d + \alpha e^{-\lambda\tau}\big) - k\alpha r e^{-\lambda\tau} = 0.$$

At the origin,

$$\Delta_0(0) = (\alpha + \mu + \varepsilon_3)\left[(\zeta + r + \mu + \varepsilon_1) - k\alpha\frac{r}{\alpha + \mu + \varepsilon_3}\right](1 - \mathcal{R}_0).$$

When $\tau = 0$, the equation becomes

$$\lambda^2 + (d + \alpha - c)\lambda - \big[c(d + \alpha) + k\alpha r\big] = 0.$$

If $\mathcal{R}_0 < 1$, then both coefficients are positive, and the Routh–Hurwitz criterion implies that both roots have negative real parts. The remaining linearized roots have negative real parts, so E_0 is locally asymptotically stable when $\tau = 0$.

If $\mathcal{R}_0 > 1$, then $\Delta_0(0) < 0$, while $\Delta_0(\lambda) \to +\infty$ as $\lambda \to +\infty$ along the real axis. Hence Δ_0 has a positive real root, and E_0 is unstable.

For $\tau > 0$, a stability boundary can occur only when $\lambda = i\omega$, $\omega > 0$. Substitution gives

$$(i\omega - c)(i\omega + d) + \alpha(i\omega - c - kr)e^{-i\omega\tau} = 0.$$

Taking moduli yields (16). Therefore, in the absence of positive roots of (16), no conjugate pair crosses the imaginary axis; stability then persists on the delay interval under consideration by continuity of characteristic roots for retarded functional differential equations [12,13]. □

5.2. **Endemic equilibrium for $\tau = 0$.** Throughout the remainder of the paper, we assume $\mathcal{R}_0 > 1$ so that the endemic equilibrium E^* exists.

Let

$$f(S, I) = \frac{\beta SI}{1 + aS + bI}.$$

At (S^*, I^*), define

$$p = \frac{\partial f}{\partial S}\bigg|_{(S^*,I^*)} = \frac{\beta I^*(1 + bI^*)}{(1 + aS^* + bI^*)^2}, \qquad q = \frac{\partial f}{\partial I}\bigg|_{(S^*,I^*)} = \frac{\beta S^*(1 + aS^*)}{(1 + aS^* + bI^*)^2}. \tag{17}$$

Set

$$a_1 = \gamma + \mu + p, \qquad c_1 = \mu + \varepsilon_3, \qquad D_0 = (\zeta + r + \mu + \varepsilon_1) - (1 - \varepsilon)\theta. \tag{18}$$

Lemma 5.2. *The characteristic equation of the linearization of* (1) *at* E^* *factors as*

$$(\lambda + \mu)(\lambda + \mu + \varepsilon_2)\Delta(\lambda, \tau) = 0, \tag{19}$$

where

$$\Delta(\lambda, \tau) = P(\lambda) + Q(\lambda)e^{-\lambda\tau}, \tag{20}$$

with

$$P(\lambda) = (\lambda + c_1)B(\lambda), \qquad Q(\lambda) = \alpha\big(B(\lambda) - kr(\lambda + a_1)\big), \tag{21}$$

and

$$B(\lambda) = (\lambda + D_0 - q)(\lambda + a_1) + pq. \tag{22}$$

Proof. Let

$$S(t) = S^* + x_1(t), \quad I(t) = I^* + x_2(t), \quad T(t) = T^* + x_3(t), \quad A(t) = A^* + x_4(t), \quad R(t) = R^* + x_5(t),$$

where $|x_j(t)|$ is small. Since

$$f(S, I) = \frac{\beta SI}{1 + aS + bI}, \qquad p = \left.\frac{\partial f}{\partial S}\right|_{(S^*, I^*)}, \qquad q = \left.\frac{\partial f}{\partial I}\right|_{(S^*, I^*)},$$

the first-order expansion of f around (S^*, I^*) is

$$f(S^* + x_1, I^* + x_2) = f(S^*, I^*) + px_1 + qx_2 + o(\|(x_1, x_2)\|).$$

Substituting the perturbation variables into (1), using the equilibrium relations satisfied by E^*, and retaining only linear terms yields

$$\begin{aligned}
x_1'(t) &= -a_1 x_1(t) - q x_2(t), \\
x_2'(t) &= p x_1(t) - (D_0 - q) x_2(t) + k\alpha x_3(t - \tau), \\
x_3'(t) &= r x_2(t) - c_1 x_3(t) - \alpha x_3(t - \tau), \\
x_4'(t) &= \zeta x_2(t) + (1 - k)\alpha x_3(t - \tau) - (\mu + \varepsilon_2) x_4(t), \\
x_5'(t) &= \gamma x_1(t) - \mu x_5(t),
\end{aligned} \tag{23}$$

where a_1, c_1, and D_0 are defined in (18).

Seeking exponential solutions of the form $x_j(t) = \xi_j e^{\lambda t}$ gives the algebraic system

$$\begin{pmatrix}
\lambda + a_1 & q & 0 & 0 & 0 \\
-p & \lambda + D_0 - q & -k\alpha e^{-\lambda\tau} & 0 & 0 \\
0 & -r & \lambda + c_1 + \alpha e^{-\lambda\tau} & 0 & 0 \\
0 & -\zeta & -(1 - k)\alpha e^{-\lambda\tau} & \lambda + \mu + \varepsilon_2 & 0 \\
-\gamma & 0 & 0 & 0 & \lambda + \mu
\end{pmatrix}
\begin{pmatrix} \xi_1 \\ \xi_2 \\ \xi_3 \\ \xi_4 \\ \xi_5 \end{pmatrix} = 0.$$

Hence, the characteristic equation is obtained by setting the determinant of the above matrix equal to zero. Because the variables x_4 and x_5 do not feed back into the (x_1, x_2, x_3) subsystem, this determinant is block triangular and factors as

$$(\lambda + \mu)(\lambda + \mu + \varepsilon_2) \det M_3(\lambda, \tau) = 0,$$

where

$$M_3(\lambda, \tau) = \begin{pmatrix}
\lambda + a_1 & q & 0 \\
-p & \lambda + D_0 - q & -k\alpha e^{-\lambda\tau} \\
0 & -r & \lambda + c_1 + \alpha e^{-\lambda\tau}
\end{pmatrix}.$$

Expanding the determinant of $M_3(\lambda,\tau)$ along the first row, we get

$$\begin{aligned}\det M_3(\lambda,\tau) &= (\lambda+a_1)\begin{vmatrix}\lambda+D_0-q & -k\alpha e^{-\lambda\tau}\\ -r & \lambda+c_1+\alpha e^{-\lambda\tau}\end{vmatrix} - q\begin{vmatrix}-p & -k\alpha e^{-\lambda\tau}\\ 0 & \lambda+c_1+\alpha e^{-\lambda\tau}\end{vmatrix}\\ &= (\lambda+a_1)\Big((\lambda+D_0-q)(\lambda+c_1+\alpha e^{-\lambda\tau}) - k\alpha r e^{-\lambda\tau}\Big) + pq(\lambda+c_1+\alpha e^{-\lambda\tau})\\ &= (\lambda+c_1+\alpha e^{-\lambda\tau})\Big((\lambda+a_1)(\lambda+D_0-q)+pq\Big) - k\alpha r(\lambda+a_1)e^{-\lambda\tau}.\end{aligned}$$

Let

$$B(\lambda) = (\lambda+a_1)(\lambda+D_0-q)+pq.$$

Then the previous identity becomes

$$\det M_3(\lambda,\tau) = (\lambda+c_1)B(\lambda) + \alpha B(\lambda)e^{-\lambda\tau} - k\alpha r(\lambda+a_1)e^{-\lambda\tau}.$$

Therefore,

$$\det M_3(\lambda,\tau) = P(\lambda) + Q(\lambda)e^{-\lambda\tau},$$

where

$$P(\lambda) = (\lambda+c_1)B(\lambda), \qquad Q(\lambda) = \alpha\big(B(\lambda) - kr(\lambda+a_1)\big).$$

This is exactly (20)–(22), and hence

$$(\lambda+\mu)(\lambda+\mu+\varepsilon_2)\Delta(\lambda,\tau) = 0.$$

□

Before introducing the zero-delay cubic, define

$$B(\lambda) = \lambda^2 + B_1\lambda + B_0, \qquad B_1 = a_1 + D_0 - q, \qquad B_0 = a_1(D_0-q)+pq. \tag{24}$$

Then

$$p_2 = B_1 + c_1, \qquad p_1 = B_0 + c_1B_1, \qquad p_0 = c_1B_0, \tag{25}$$

and

$$q_1 = B_1 - kr, \qquad q_0 = B_0 - kra_1. \tag{26}$$

When $\tau = 0$, the reduced characteristic equation becomes the cubic polynomial

$$H(\lambda) = \Delta(\lambda,0) = \lambda^3 + h_2\lambda^2 + h_1\lambda + h_0,$$

where

$$h_2 = p_2 + \alpha, \qquad h_1 = p_1 + \alpha q_1, \qquad h_0 = p_0 + \alpha q_0, \tag{27}$$

after writing

$$P(\lambda) = \lambda^3 + p_2\lambda^2 + p_1\lambda + p_0, \qquad Q(\lambda) = \alpha(\lambda^2 + q_1\lambda + q_0). \tag{28}$$

Theorem 5.3. *Assume $\mathcal{R}_0 > 1$ and let E^* be the endemic equilibrium. If*

$$h_2 > 0, \qquad h_1 > 0, \qquad h_0 > 0, \qquad h_2 h_1 > h_0, \tag{29}$$

then E^* is locally asymptotically stable when $\tau = 0$. Moreover, there exists $\tau^\dagger > 0$ such that E^* remains locally asymptotically stable for all $0 \le \tau < \tau^\dagger$.

Proof. Setting $\tau = 0$ in (20) gives

$$\Delta(\lambda, 0) = P(\lambda) + Q(\lambda) =: H(\lambda).$$

Using (24), we first write

$$B(\lambda) = \lambda^2 + B_1\lambda + B_0.$$

Hence, by (21),

$$P(\lambda) = (\lambda + c_1)B(\lambda) = \lambda^3 + (B_1 + c_1)\lambda^2 + (B_0 + c_1 B_1)\lambda + c_1 B_0,$$

and

$$Q(\lambda) = \alpha\big(B(\lambda) - kr(\lambda + a_1)\big) = \alpha\big(\lambda^2 + (B_1 - kr)\lambda + (B_0 - kra_1)\big).$$

Therefore,

$$H(\lambda) = \lambda^3 + h_2\lambda^2 + h_1\lambda + h_0,$$

with

$$h_2 = p_2 + \alpha, \qquad h_1 = p_1 + \alpha q_1, \qquad h_0 = p_0 + \alpha q_0,$$

as stated in (27). By Lemma 5.2, the full characteristic equation at $\tau = 0$ is

$$(\lambda + \mu)(\lambda + \mu + \varepsilon_2)H(\lambda) = 0.$$

Thus, the delay-independent roots $-\mu$ and $-(\mu + \varepsilon_2)$ are already strictly negative, and the local stability of E^* is determined entirely by the cubic factor $H(\lambda)$.

We now apply the Routh–Hurwitz criterion for a cubic polynomial. For

$$H(\lambda) = \lambda^3 + h_2\lambda^2 + h_1\lambda + h_0,$$

all roots satisfy $\Re(\lambda) < 0$ if and only if

$$h_2 > 0, \qquad h_1 > 0, \qquad h_0 > 0, \qquad h_2 h_1 > h_0.$$

These are exactly the conditions in (29). Hence, every root of $H(\lambda)$ lies in the open left half-plane. Combining this with the two fixed roots $-\mu$ and $-(\mu + \varepsilon_2)$, we conclude that all characteristic roots of the linearized system have negative real parts. Therefore, the endemic equilibrium E^* is locally asymptotically stable when $\tau = 0$.

To establish persistence, let

$$\eta = \frac{1}{2}\min\Big\{\mu, \mu+\varepsilon_2,\ -\max\{\Re\lambda :\ H(\lambda)=0\}\Big\} > 0.$$

The quantity η is well defined because the previous part shows that every root of H has strictly negative real part. Characteristic roots of retarded functional differential equations depend continuously on the delay parameter ([12], [13]). Consequently, for sufficiently small $\tau \geq 0$, the roots of

$$(\lambda+\mu)(\lambda+\mu+\varepsilon_2)\Delta(\lambda,\tau) = 0$$

remain inside the half-plane $\Re(\lambda) < -\eta$. In particular, there exists $\tau^\dagger > 0$ such that no characteristic root crosses the imaginary axis for $0 \leq \tau < \tau^\dagger$. It follows from the linearized stability principle that E^* remains locally asymptotically stable for all $0 \leq \tau < \tau^\dagger$. □

6. Hopf bifurcation induced by the treatment delay

To determine when the endemic equilibrium loses stability, we look for purely imaginary roots of (20). We use the notation introduced in (24)–(26).

Lemma 6.1. *Let $\omega > 0$ and set $\lambda = i\omega$. Then $\lambda = i\omega$ is a root of (20) for some $\tau \geq 0$ if and only if*

$$|P(i\omega)| = |Q(i\omega)|. \tag{30}$$

Whenever (30) holds, the corresponding critical delays are

$$\tau_n = \frac{1}{\omega}\left(2n\pi - \arg\left(-\frac{P(i\omega)}{Q(i\omega)}\right)\right), \qquad n = 0,1,2,\ldots, \tag{31}$$

where the branch of the argument is chosen so that $\tau_n > 0$.

Proof. Substituting $\lambda = i\omega$ into (20) gives

$$P(i\omega) + Q(i\omega)e^{-i\omega\tau} = 0 \iff e^{-i\omega\tau} = -\frac{P(i\omega)}{Q(i\omega)}.$$

Because the left-hand side has modulus one, the equality can hold only when (30) is satisfied. Once (30) holds, taking arguments on both sides yields

$$-\omega\tau = \arg\left(-\frac{P(i\omega)}{Q(i\omega)}\right) + 2m\pi, \qquad m \in \mathbb{Z},$$

which is equivalent to (31) after relabeling the integer index to obtain positive delays. □

For computation, condition (30) can be rewritten as an equation in $u = \omega^2$. Indeed,

$$P(i\omega) = (p_0 - p_2\omega^2) + i\omega(p_1 - \omega^2), \qquad Q(i\omega) = \alpha\big((q_0 - \omega^2) + iq_1\omega\big),$$

so (30) becomes

$$(p_0 - p_2 u)^2 + u(p_1 - u)^2 - \alpha^2\big((q_0 - u)^2 + q_1^2 u\big) = 0, \qquad u = \omega^2 > 0. \tag{32}$$

Let

$$\Phi(u) = (p_0 - p_2u)^2 + u(p_1 - u)^2 - \alpha^2 \left[(q_0 - u)^2 + q_1^2 u\right].$$

Theorem 6.2. *Assume that E^* exists and is locally asymptotically stable at $\tau = 0$. Suppose that $\Phi(u) = 0$ has a positive simple root $u^* = (\omega^*)^2$, that is,*

$$\Phi(u^*) = 0, \qquad \Phi'(u^*) \neq 0,$$

and assume that $P(i\omega^*)Q(i\omega^*) \neq 0$. Let τ_n be defined by (31). Suppose further that no other characteristic roots lie on the imaginary axis at $\tau = \tau_n$. Then $\lambda = \pm i\omega^*$ are simple characteristic roots and cross the imaginary axis with nonzero speed at $\tau = \tau_n$. Consequently, system (1) undergoes a Hopf bifurcation at E^* when τ passes through τ_n.

Proof. Since $\Phi(u^*) = 0$ and $u^* = (\omega^*)^2 > 0$, we have

$$|P(i\omega^*)| = |Q(i\omega^*)|.$$

By Lemma 6.1, there exists a sequence of critical delays τ_n such that

$$\Delta(i\omega^*, \tau_n) = 0.$$

Hence $\lambda = i\omega^*$ is a characteristic root at $\tau = \tau_n$. Since the characteristic equation has real coefficients, $\lambda = -i\omega^*$ is also a characteristic root.

We first show that these roots are simple. Let

$$A(\omega) = P(i\omega), \qquad B(\omega) = Q(i\omega), \qquad E(\omega) = e^{-i\omega\tau_n}.$$

At $\omega = \omega^*$, the characteristic equation gives

$$A(\omega^*) + B(\omega^*)E(\omega^*) = 0.$$

Suppose, on the contrary, that $\lambda = i\omega^*$ is not a simple root. Then

$$\Delta_\lambda(i\omega^*, \tau_n) = 0.$$

Equivalently,

$$\frac{d}{d\omega}\left[A(\omega) + B(\omega)E(\omega)\right]_{\omega=\omega^*} = 0.$$

Using $A(\omega^*) = -B(\omega^*)E(\omega^*)$, this implies

$$\frac{d}{d\omega}\left(|A(\omega)|^2 - |B(\omega)|^2\right)_{\omega=\omega^*} = 0.$$

But

$$|A(\omega)|^2 - |B(\omega)|^2 = \Phi(\omega^2).$$

Therefore,

$$0 = \frac{d}{d\omega}\Phi(\omega^2)\Big|_{\omega=\omega^*} = 2\omega^*\Phi'(u^*).$$

Since $\omega^* > 0$ and $\Phi'(u^*) \neq 0$, this is a contradiction. Thus $\lambda = i\omega^*$ is a simple characteristic root. By conjugacy, $\lambda = -i\omega^*$ is also simple.

It remains to verify the transversality condition. Differentiating

$$\Delta(\lambda, \tau) = P(\lambda) + Q(\lambda)e^{-\lambda\tau} = 0$$

with respect to τ gives

$$\frac{d\lambda}{d\tau} = \frac{\lambda Q(\lambda)e^{-\lambda\tau}}{P'(\lambda) + e^{-\lambda\tau}\left(Q'(\lambda) - \tau Q(\lambda)\right)}.$$

Taking the reciprocal and using

$$e^{-\lambda\tau} = -\frac{P(\lambda)}{Q(\lambda)}$$

at the critical root gives

$$\left(\frac{d\lambda}{d\tau}\right)^{-1} = -\frac{P'(\lambda)}{\lambda P(\lambda)} + \frac{Q'(\lambda)}{\lambda Q(\lambda)} - \frac{\tau}{\lambda}.$$

At $\lambda = i\omega^*$, the last term is purely imaginary. Hence

$$\Re\left[\left(\frac{d\lambda}{d\tau}\right)^{-1}\right]_{\lambda=i\omega^*} = \frac{1}{2\omega^*|P(i\omega^*)|^2}\frac{d}{d\omega}\left(|P(i\omega)|^2 - |Q(i\omega)|^2\right)_{\omega=\omega^*}.$$

Since

$$|P(i\omega)|^2 - |Q(i\omega)|^2 = \Phi(\omega^2),$$

we obtain

$$\Re\left[\left(\frac{d\lambda}{d\tau}\right)^{-1}\right]_{\lambda=i\omega^*} = \frac{\Phi'(u^*)}{|P(i\omega^*)|^2}.$$

Because $\Phi'(u^*) \neq 0$ and $P(i\omega^*) \neq 0$, it follows that

$$\Re\left[\left(\frac{d\lambda}{d\tau}\right)^{-1}\right] \neq 0.$$

Therefore,

$$\Re\left(\frac{d\lambda}{d\tau}\right) \neq 0.$$

Thus, the pair $\lambda = \pm i\omega^*$ crosses the imaginary axis with nonzero speed as τ passes through τ_n.

Since E^* is locally asymptotically stable at $\tau = 0$, and since no other characteristic roots lie on the imaginary axis at $\tau = \tau_n$, the Hopf bifurcation theorem for retarded functional differential equations implies that system (1) undergoes a Hopf bifurcation at E^* when τ passes through τ_n. □

7. Numerical simulations and sensitivity analysis

This section illustrates the theoretical results using representative parameter sets. The parameter values are used for qualitative exploration rather than data fitting. All numerical simulations were carried out in Python with initial histories taken to be constants and equal to the prescribed initial state on $[-\tau, 0]$, and the simulations were performed over the indicated time intervals using the parameter values in Table 2. To illustrate the local stability results in Theorems 5.1 and 5.3, we first set $\tau = 0$ and implement the corresponding ODE system. We then return to the delayed model to illustrate the stability switch and Hopf bifurcation mechanism.

7.1. **Local stability results.**

We first illustrate Theorem 5.1. Starting from the baseline values in Table 2, we reduce the horizontal-transmission parameter to

$$\beta = 0.005,$$

while keeping $\theta = 0.0400$ and the remaining parameters unchanged. For this modified set,

$$\mathcal{R}_0 \approx 0.9462 < 1,$$

so the disease-free equilibrium is locally asymptotically stable. Since

$$S_0 = \frac{\pi}{\gamma + \mu} \approx 142.8571, \qquad R_0 = \frac{\gamma}{\mu} S_0 \approx 357.1429,$$

the corresponding disease-free state is

$$E_0 \approx (142.8571,\ 0,\ 0,\ 0,\ 357.1429).$$

Using the initial condition

$$(S(0), I(0), T(0), A(0), R(0)) = (140, 10, 5, 2, 350),$$

Figure 2(a) shows that the infectious, treated, and AIDS classes decay toward zero, in agreement with Theorem 5.1. Because the threshold value is close to one, the decay is gradual.

To illustrate Theorem 5.3, we return to the baseline parameter set in Table 2 and set $\tau = 0$. In this case,

$$\mathcal{R}_0 \approx 32.7348 > 1,$$

and the endemic equilibrium computed from (11)–(13) is

$$E^* \approx (1.1187,\ 83.4910,\ 80.9911,\ 162.5683,\ 2.7967).$$

Choosing a nearby initial point,

$$(S(0), I(0), T(0), A(0), R(0)) = (1.07S^*,\ 0.92I^*,\ 1.08T^*,\ 0.90A^*,\ 1.05R^*),$$

Figure 2(b) shows convergence of the infectious variables toward their endemic levels. This confirms the local asymptotic stability of E^* when the delay is absent.

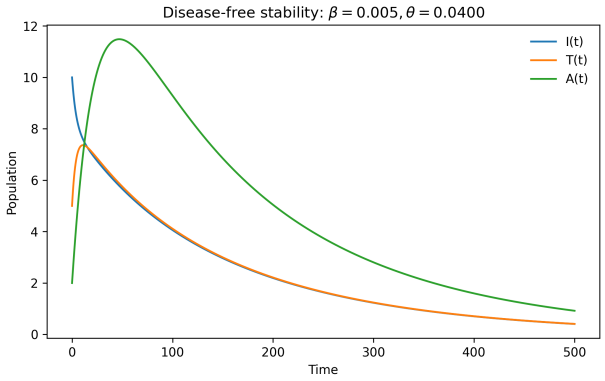

(A) Decay to the disease-free equilibrium when $\mathcal{R}_0 < 1$.

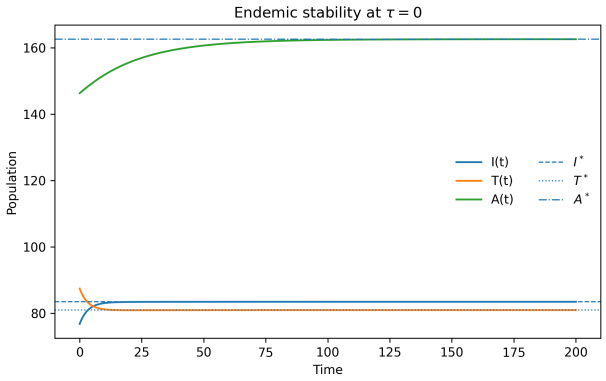

(B) Convergence to the endemic equilibrium when $\tau = 0$.

FIGURE 2. Numerical illustrations of the local stability results in Theorems 5.1 and 5.3.

7.2. **Baseline parameter set.** Table 2 lists the baseline values used throughout the numerical section.

TABLE 2. Baseline parameter values used in the numerical illustrations.

π	μ	γ	β	a	b	ε	θ
10	0.02	0.05	0.2314	0.0383	0.0136	0.0404	0.0400
ζ	r	ε_1	ε_2	ε_3	α	k	
0.0487	0.1500	0.0262	0.0237	0.00673	0.1279	0.7067	

For the same parameter set,

$$\mathcal{R}_0 \approx 32.7348 > 1.$$

Hence, by Theorem 4.2, the system admits a unique positive endemic equilibrium. Using (11) and (9), we obtain

$$E^* \approx (1.1187,\ 83.4910,\ 80.9911,\ 162.5683,\ 2.7967).$$

For the same baseline, $c = \mu + \varepsilon_3 = 0.02673$ and $\alpha = 0.1279$. Thus, the sufficient first-step condition (4) gives

$$\tau \leq \frac{1}{c} \ln\left(1 + \frac{c}{\alpha}\right) \approx 7.10.$$

The delays used in the Hopf simulations exceed this sufficient first-step bound. Therefore, the delayed simulations are interpreted as numerical explorations under the chosen admissible histories. In the displayed simulations, the computed trajectories remained nonnegative.

At $\tau = 0$, the cubic coefficients in (27) are

$$h_2 \approx 9.0689, \qquad h_1 \approx 3.1709, \qquad h_0 \approx 0.1604,$$

and

$$h_2 h_1 - h_0 \approx 28.5965 > 0.$$

Hence, the Routh–Hurwitz conditions in Theorem 5.3 are satisfied and the endemic equilibrium is stable when the delay is absent.

Solving (32) for the baseline parameter set gives one positive root,

$$u_1 \approx 0.00427170,$$

corresponding to

$$\omega_1 \approx 0.0653583.$$

The smallest positive critical delay is

$$\tau_c \approx 34.1108.$$

At this critical value,

$$\Re\left(\frac{d\lambda}{d\tau}\Big|_{\lambda=i\omega_1,\,\tau=\tau_c}\right) \approx 4.46 \times 10^{-4} > 0,$$

which confirms transversality. Thus, the conjugate pair crosses from the left half-plane to the right half-plane as τ increases through τ_c. This value acts as a stability threshold: below τ_c, the endemic equilibrium attracts nearby solutions; beyond τ_c, the delay is large enough to generate oscillatory behavior.

7.3. **Delay-driven dynamics.** To visualize the effect of the delay, we perturb the endemic equilibrium and simulate the infectious class for three representative cases: $\tau = 20 < \tau_c$, $\tau = 34.11 \approx \tau_c$, and $\tau = 40 > \tau_c$.

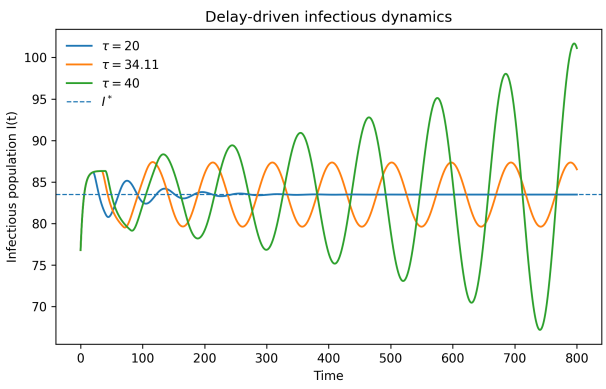

(A) Time series of the infectious class under different delays.

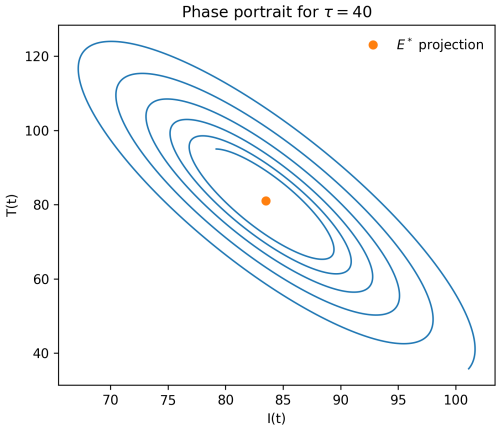

(B) Phase portrait $(I(t), T(t))$ for $\tau = 40$.

FIGURE 3. Delay-induced stability switch at the endemic equilibrium.

Figure 3(a) confirms the theoretical results. When $\tau = 20$, the infectious class returns to the endemic equilibrium after the initial perturbation. Near the threshold, at $\tau = 34.11$, the decay becomes weak and oscillations persist over a long time scale. For a larger delay, $\tau = 40$, the oscillations become more pronounced. This is reinforced by Figure 3(b), where the trajectory in the (I, T)-plane spirals away from the endemic projection instead of collapsing rapidly to a point. Biologically, this means that a long treatment-completion delay can destabilize a steady endemic burden and produce recurrent waves of infection and treatment load.

7.4. **Additional scenario analysis.** To complement the delay experiment, we also compare several intervention-oriented scenarios using the same model structure and a moderate delay $\tau = 20$. The initial history is chosen close to the disease-free state so that the trajectories describe an outbreak phase rather than small perturbations around the endemic equilibrium.

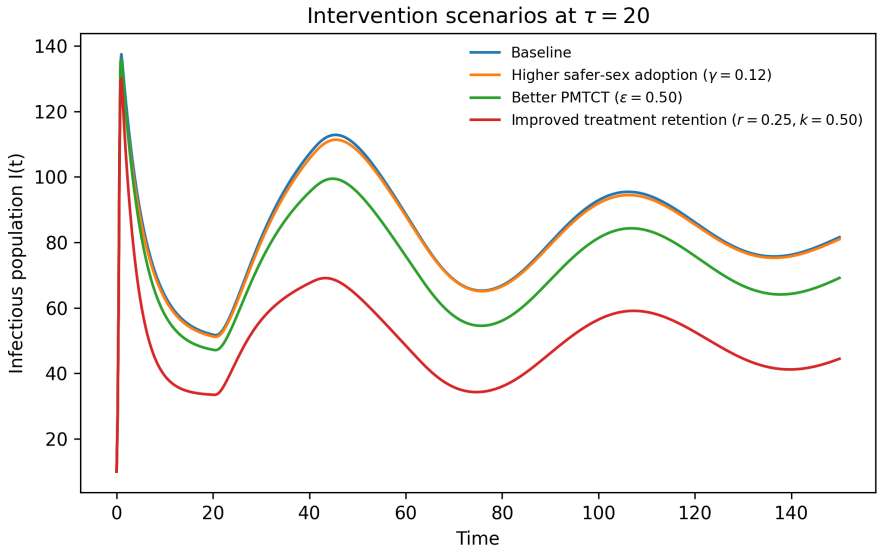

FIGURE 4. Outbreak trajectories under selected intervention scenarios.

The comparison in Figure 4 suggests that not all control measures act with the same intensity under the chosen baseline. Increasing the safer-sex transition rate from $\gamma = 0.05$ to $\gamma = 0.12$ produces only a slight reduction in the infectious trajectory. Increasing the effectiveness of prevention of mother-to-child transmission from $\varepsilon = 0.0404$ to $\varepsilon = 0.50$ produces a clearer reduction, although its effect is now more moderate because the recomputed baseline uses the smaller value $\theta = 0.0400$. The largest decline is observed when treatment retention is improved by simultaneously increasing the treatment rate to $r = 0.25$ and reducing the return fraction to $k = 0.50$. At time $t = 150$, the infectious level falls from about 81.58 in the baseline case to 80.95 under higher safer-sex adoption, to 69.14 under better PMTCT, and to 44.46 under improved treatment retention.

These scenarios highlight two insights. First, treatment-related parameters can reshape the short-term and medium-term outbreak profile even when the endemic threshold remains above one. Second, vertical transmission control remains protective, but its local and scenario-level effect is smaller when the baseline vertical-transmission potential is reduced.

7.5. **Local sensitivity analysis.** To assess parameter influence near the baseline configuration, we use the normalized forward sensitivity index

$$\Upsilon_p^{\mathcal{R}_0} = \frac{\partial \mathcal{R}_0}{\partial p} \cdot \frac{p}{\mathcal{R}_0}, \tag{33}$$

which measures the relative change in $\mathcal{R}_0$ caused by a relative change in the parameter p.

For the numerator

$$A = \frac{\beta\pi}{\gamma + \mu + a\pi} + (1-\varepsilon)\theta$$

and denominator

$$B = (\zeta + r + \mu + \varepsilon_1) - k\alpha\frac{r}{\alpha + \mu + \varepsilon_3},$$

we have $\mathcal{R}_0 = A/B$. Thus, for example,

$$\Upsilon_\beta^{\mathcal{R}_0} = \frac{\beta\pi}{(\gamma + \mu + a\pi)A}, \qquad \Upsilon_\theta^{\mathcal{R}_0} = \frac{(1-\varepsilon)\theta}{A}, \qquad \Upsilon_\varepsilon^{\mathcal{R}_0} = -\frac{\varepsilon\theta}{A}.$$

The remaining indices were evaluated numerically at the baseline parameter set. The resulting values are

$$\Upsilon_\beta^{\mathcal{R}_0} \approx 0.993, \quad \Upsilon_k^{\mathcal{R}_0} \approx 0.558, \quad \Upsilon_r^{\mathcal{R}_0} \approx -0.396, \quad \Upsilon_\mu^{\mathcal{R}_0} \approx -0.243,$$

$$\Upsilon_\gamma^{\mathcal{R}_0} \approx -0.110, \quad \Upsilon_\alpha^{\mathcal{R}_0} \approx 0.096, \quad \Upsilon_\theta^{\mathcal{R}_0} \approx 0.007, \quad \Upsilon_\varepsilon^{\mathcal{R}_0} \approx -0.0003.$$

Table 3 summarizes the signs and interpretations of the local sensitivity indices computed using formula (33). The small indices for θ and ε are specific to the baseline values $\theta = 0.0400$ and $\varepsilon = 0.0404$, and therefore should be interpreted only as local, parameter-dependent results rather than as evidence that vertical-transmission control is biologically unimportant.

TABLE 3. Interpretation of selected local sensitivity indices at the baseline parameter set.

Parameter	Baseline value	Sign	Interpretation
β	0.2314	$+$	Higher transmission increases $\mathcal{R}_0$.
k	0.7067	$+$	More return to infectiousness increases $\mathcal{R}_0$.
r	0.1500	$-$	Faster treatment initiation lowers $\mathcal{R}_0$.
μ	0.0200	$-$	Higher removal through natural mortality lowers the threshold.
γ	0.0500	$-$	Safer-sex transition reduces transmission opportunity.
α	0.1279	$+$	Faster completion can increase return flow when $k > 0$.
θ	0.0400	$+$	Stronger vertical transmission increases $\mathcal{R}_0$.
ε	0.0404	$-$	Improved PMTCT lowers vertical transmission.

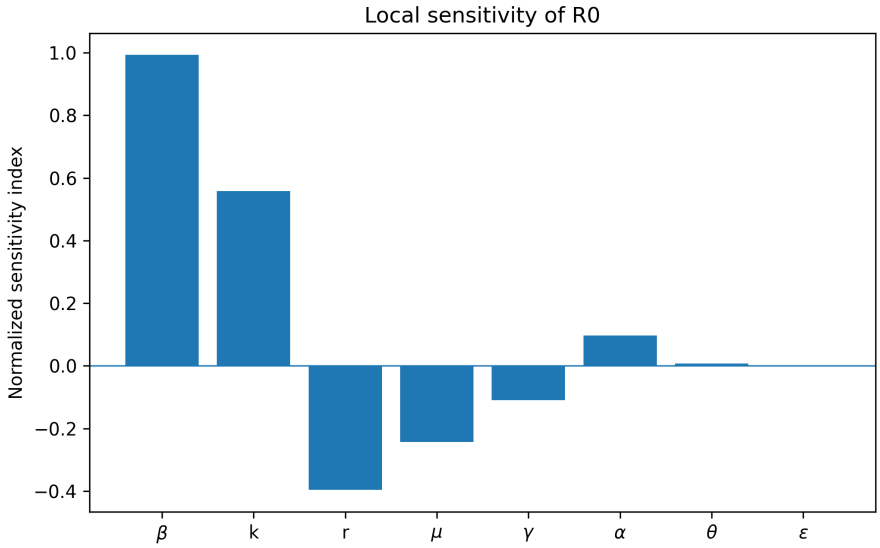

FIGURE 5. Normalized local sensitivity indices of $\mathcal{R}_0$ at the baseline parameter set.

Figure 5 shows that the transmission rate β is the most influential positive parameter near the baseline point. A 1% increase in β produces almost a 0.99% increase in $\mathcal{R}_0$. The return fraction k is also highly influential, which underscores the epidemiological importance of treatment failure or relapse into infectiousness. On the other hand, the negative index for r indicates that increasing treatment initiation lowers the threshold, while the negative index for γ reflects the protective role of behavior change toward safer sexual practices.

Practically, the dominant parameters may suggest control directions: reducing β through transmission-prevention measures, lowering k by preventing loss of viral suppression among treated individuals, increasing r through early treatment initiation, and increasing γ through safer-sex behavior interventions. Hence, a combined strategy involving prevention education, safer-sex promotion, early treatment enrollment, adherence support, and sustained linkage to care is expected to be effective in lowering $\mathcal{R}_0$.

8. CONCLUSION

We studied an HIV/AIDS model with vertical transmission, saturated incidence, safer-sex behavior, and a discrete delay in treatment completion. The analysis showed that the threshold quantity $\mathcal{R}_0$ characterizes the zero-growth invasion threshold of the infected subsystem and the existence of the endemic equilibrium under the stated assumptions. At the endemic state, the linearized problem reduces to a characteristic equation of the form $P(\lambda) + Q(\lambda)e^{-\lambda\tau} = 0$, which shows how the treatment-completion delay influences local stability and may generate Hopf bifurcation.

The numerical simulations make the analytical conclusions easier to interpret. For the recomputed baseline with $\theta = 0.0400$, the endemic equilibrium is stable when the delay is small, but a Hopf bifurcation occurs at approximately $\tau_c = 34.11$, after which oscillatory instability is observed in the numerical simulations. This means that long treatment-completion delays can destabilize a steady chronic burden and generate recurrent epidemic waves. The additional scenarios further indicate that improving treatment retention is especially effective in reducing the infectious burden under the chosen baseline, while strengthening PMTCT remains protective but produces a more moderate effect because the vertical-transmission potential has been reduced. The sensitivity results does not only confirm the expected role of the transmission rate β, but more importantly highlight actionable control targets. Reducing loss of viral suppression among treated individuals, increasing treatment initiation, and strengthening safer sexual behavior may substantially lower the epidemic threshold and are important for controlling the long-term dynamics of HIV/AIDS.

A direction for further work is to refine the treatment-completion mechanism so that positivity is guaranteed for all biologically admissible histories, or to develop sharper invariant-set conditions for the present delayed-loss formulation, especially for delays beyond the sufficient bound used in the well-posedness argument.

Author Contributions. The sole author initiated the study, carried out the mathematical analysis, performed the numerical experiments, and wrote and revised the manuscript.

Conflicts of Interest. The author declares that there is no conflict of interest regarding the publication of this paper.

References

[1] D. Wang, Y. Liu, X. Gao, C. Wang, D. Fan, Dynamics of an HIV Infection Model with Two Time Delays, Discret. Contin. Dyn. Syst. B 28 (2023), 5641–5661. https://doi.org/10.3934/dcdsb.2023069.

[2] P. Wu, R. Zhang, A. Din, Mathematical Analysis of an Age-since Infection and Diffusion HIV/AIDS Model with Treatment Adherence and Dirichlet Boundary Condition, Math. Comput. Simul. 214 (2023), 1–27. https://doi.org/10.1016/j.matcom.2023.06.018.

[3] L. Zhang, J. Wang, R. Zhang, Mathematical Analysis for an Age-Space Structured HIV Model with Latency, Math. Comput. Simul. 220 (2024), 595–617. https://doi.org/10.1016/j.matcom.2024.02.017.

[4] Z. Chazuka, E. Mudimu, D. Mathebula, Stability and Bifurcation Analysis of an HIV Model with Pre-exposure Prophylaxis and Treatment Interventions, Sci. Afr. 23 (2024), e01979. https://doi.org/10.1016/j.sciaf.2023.e01979.

[5] N.H. AlShamrani, R.H. Halawani, A.M. Elaiw, Stability of Generalized Models for HIV-1 Dynamics with Impaired CTL Immunity and Three Pathways of Infection, Front. Appl. Math. Stat. 10 (2024), 1412357. https://doi.org/10.3389/fams.2024.1412357.

[6] B. Lahmidani, Y. Tabit, O. Baiz, D. El Moutawakil, Mathematical Analysis of an HIV Model with Two Saturated Rates, CTL Response and Therapy, Asia Pac. J. Math. 10 (2023), 49. https://doi.org/10.28924/APJM/10-49.

[7] Y. Li, L. Zhang, J. Zhang, S. Liu, Z. Peng, Dynamical Modeling and Data Analysis of HIV Infection with Infection-Age, CTLs Immune Response and Delayed Antibody Immune Response, J. Math. Biol. 91 (2025), 57. https://doi.org/10.1007/s00285-025-02285-y.

[8] M. Marsudi, T. Trisilowati, R.R. Musafir, Bifurcation and Optimal Control Analysis of an HIV/AIDS Model with Saturated Incidence Rate, Mathematics 13 (2025), 2149. https://doi.org/10.3390/math13132149.

[9] A.E. Sado, G.F. Duressa, C.T. Deressa, Mathematical Modeling of HIV/AIDS Dynamics with Optimal Control Analysis, Sci. Afr. 30 (2025), e02972. https://doi.org/10.1016/j.sciaf.2025.e02972.

[10] T.R.Y. Teng, E.P. De Lara-Tuprio, J.M.R. Macalalag, An HIV/AIDS Epidemic Model with Media Coverage, Vertical Transmission and Time Delays, AIP Conf. Proc. 2192 (2019), 060021. https://doi.org/10.1063/1.5139167.

[11] P. van den Driessche, J. Watmough, Reproduction Numbers and Sub-threshold Endemic Equilibria for Compartmental Models of Disease Transmission, Math. Biosci. 180 (2002), 29–48. https://doi.org/10.1016/S0025-5564(02)00108-6.

[12] J.K. Hale, S.M.V. Lunel, Introduction to Functional Differential Equations, Springer New York, 1993. https://doi.org/10.1007/978-1-4612-4342-7.

[13] Y. Kuang, Delay Differential Equations with Applications in Population Dynamics, Academic Press, 1993. https://doi.org/10.1016/s0076-5392(08)x6164-8.